*Phys. Chem. Glasses*, 2001, **42** (3), 255–64

# Investigation of lithium chloride–lithium borate–tellurium dioxide glasses: an example of complex anionic speciation

*K. J. Rao*[1] *& M. Harish Bhat*

*Solid State and Structural Chemistry Unit, Indian Institute of Science, Bangalore - 560 012, India*

*Glasses in the system lithium chloride–lithium borate–tellurium dioxide have been prepared by the melt quenching route and characterised for their densities, glass transition temperatures and heat capacities. Their structures have been investigated using infrared, Raman and magic angle spinning nuclear magnetic resonance spectroscopies. While the structure consists of trigonal and tetrahedral borate groups, the tetrahedral boron in these glasses reaches much higher concentrations than in binary borate glasses. Tellurite species are present in both trigonal bipyramidal and trigonal pyramidal structures. The actual concentrations of the two borate and two tellurite species are interdependent. Their concentrations are also influenced by LiCl in the glass. The nature of speciation and chemical origin of the equilibration of the various species is examined using a structural model. The model has been used to rationalise the variation of the different properties in the glass system.*

In this paper we report investigations on borotellurite glasses modified by $Li_2O$ in such a way that it formally corresponds to a pseudo-binary system consisting of $LiBO_2$ and $TeO_2$. We also report studies on pseudo-ternary, $LiCl–LiBO_2–TeO_2$ glasses. These glasses, which form relatively easily from melt quenching, are rather interesting from a structural point of view, because the components of this glass, namely alkali tellurites and alkali borates themselves, exhibit unique structural features associated with borate and tellurite units. The pseudo binary $LiBO_2–TeO_2$ glasses should therefore be expected to exhibit rich and complex equilibria between structural species.

Tellurite glasses have been studied fairly extensively because of their potential application as laser hosts and as nonlinear optical materials.[1–4] $TeO_2$ by itself is traditionally considered as a conditional glass former and it forms glasses in combination with a variety of other oxide materials[5–11] such as $B_2O_3$, $V_2O_5$, $WO_3$, PbO, ZnO, $Ag_2O$ and alkalis. The Te–O bond is more covalent than the Si–O bond on the basis of Pauling electronegativity differences.

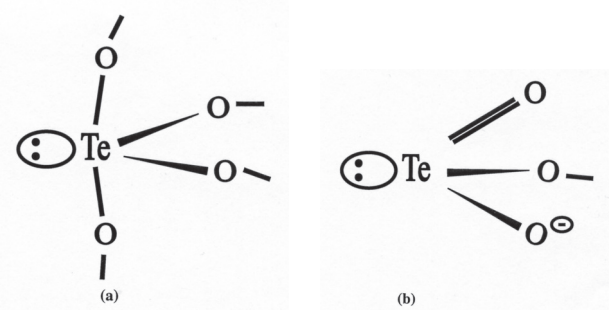


***Figure 1.*** *Structure units of (a) $TeO_4$ trigonal bipyramid (*tbp*) and (b) $TeO_3$ trigonal pyramid (*tp*) in tellurite glasses*

In $TeO_2$ Te is quadrivalent and therefore has a lone pair of electrons in the valence shell. This lone pair is generally considered to be present in one of the $sp^3d$ hybridised orbitals. In crystalline $\alpha$-$TeO_2$, Te is four coordinated to oxygen atoms forming a structural unit, $[TeO_{4/2}]^0$. $[TeO_{4/2}]^0$ is a trigonal bipyramid (*tbp*) as shown schematically in Figure 1(a). In several tellurites,[12] however, Te is also present in a trigonal pyramid (*tp*) structure (Figure 1 (b)) and is coordinated to just three oxygens, one of which is necessarily double bonded to Te. It is again required that the lone pair in Te be accommodated in a suitably hybridised orbital.[13,14] Therefore, one would expect tellurite glasses to be capable of forming extensive 3-dimensional network based on $[TeO_{4/2}]^0$ units. However, uncharged trigonal pyramidal $[TeO_{2/2}O]^0$ units would lead to glass structure based on polymeric chains.

Several structural studies using x-ray diffraction,[15–17] extended x-ray absorption fine structure (EXAFS),[18,19] x-ray photoelectron spectroscopy (XPS),[20,21] Raman[21–9] and infrared[12,30–32] spectroscopies have all revealed the presence of both *tbp* and *tp* units in tellurite glass structures. However, EXAFS investigation, which addresses the local structure more directly seems to indicate the presence of only four coordinated (*tbp*) tellurite units in glasses.[15,19] Another interesting aspect of the structure of tellurite glasses is that the addition of modifier oxides seem to favour the formation of *tp* units at the expense of *tbp* units.[5–11]

Borate glasses also exhibit well-known and unique structural features particularly in binary alkali borate glasses. The glass structures consist of three coordinated trigonal ($B_3$) and four coordinated tetrahedral

[1] Author to whom correspondence should be addressed. (e-mail: kjrao@sscu.iisc.ernet.in)

($B_4$) boron atoms. Tetrahedral borons are products of modification by the alkali. Combination of tetrahedral and trigonal borons gives rise to several unique borate species in glass such as modified boroxol, di-, tri-, tetra- and pentaborates.[33,34] The trigonal to tetrahedral conversion, and formation of oxygen bridges by the oxide ion from the modifier reaches a maximum at the diborate composition ($Li_2O/B_2O_3$=0·5). The ratio $N_4=[B_4]/\{[B_3+B_4]\}$ is around 0·5 for this composition. When the modifier concentration is increased further ($Li_2O/B_2O_3$>0·5), the percentage of tetrahedral boron decreases indicating a structural instability of tetrahedra in the presence of higher modifier oxide concentrations.[35–8] The notable feature is that there is no nonbridging oxygen (NBO) in the coordination of tetrahedral boron. The present glass system contains $LiBO_2$ where the $Li_2O/B_2O_3$ ratio is unity. The percentage of tetrahedral boron for this composition of $Li_2O$–$B_2O_3$ is expected to be much lower from a number of literature reports.[36,39–41] In the ternary $Li_2O$–$B_2O_3$–$TeO_2$ glass in which $TeO_2$ is present, this value can be higher only if the modifier $Li_2O$ is partially taken up by $TeO_2$, thereby pushing the $Li_2O/B_2O_3$ ratio to lower values (towards diborate) because tetrahedral borons can once again move up towards its value in diborate glass. It has been noted that binary $B_2O_3$–$TeO_2$ glass itself possesses a significant percentage of tetrahedral borons in the structure. It leads to speculation that $TeO_2$ itself may act as a modifier. There is an increase in *tp* tellurium units also which is surprising because concentration of *tp* generally goes up as a result of adding a modifier to $TeO_2$.

In view of the above structural aspects of $TeO_2$ and $LiBO_2$ glasses, we consider that an investigation of pseudo-binary $LiBO_2$–$TeO_2$ system of glasses would be very interesting. We have also examined the influence of the addition of LiCl to this system because we expect LiCl to open up the glass structure and stretch out the network forming elements, without itself chemically interfering with the network. This may reveal the influence of the ionicity of the environment on *tp–tbp* equilibrium of tellurite units. The behaviour of LiCl as a plasticiser in these glasses has been investigated elsewhere.[42] The addition of LiCl introduces weaker, non-bonded and noncoulombic interactions into the >B–O–Te⩽ network which is unimportant for our considerations here.

In this paper, we have studied 19 different compositions of glasses whose molar volumes, glass transition temperatures, heat capacities, infrared, Raman and $^{11}B$ HRMAS NMR spectra have been examined. In the following sections we present and discuss our experimental measurements and propose a structural model of borotellurite glasses, consisting of two network competitors for modifier oxygen, and show that it is consistent with the experimental observations.

## Experimental

Glasses were obtained using high purity commercial powders of $TeO_2$, LiCl and $LiBO_2.2H_2O$. Mixtures of these materials in appropriate proportions, Table 1, were taken in porcelain crucibles and slowly heated from 535 to 823 K (to remove water from $LiBO_2.2H_2O$) for 2 h. The resulting mixture was melted at 1223 K for 30 min and the melt was quenched between polished stainless steel plates. The amorphous nature of the samples was confirmed using x-ray diffraction (JEOL JOX-8P x-ray diffractometer). The densities of the glass pieces, free of air bubbles and cracks (visual examination), were determined through the apparent weight loss method in xylene. The molar volumes were calculated using the relation $V_M=W_M$/density where $W_M$ are the corresponding formula weights. The glass transition temperatures ($T_g$) were determined using a differential scanning calorimeter (Perkin-Elmer DSC-2) employing dry nitrogen as purge gas.

**Table 1**. *Codes, compositions, densities, molar volumes and glass transition temperatures of $LiCl$–$LiBO_2$–$TeO_2$ glasses*

| *Code* | *Composition* | *Density ($g/cm^3$)* | *Molar volume ($cm^3/mol$)* | $T_g$ *(K)* |
|---|---|---|---|---|
| BT0 | $100LiBO_2$–$0TeO_2$ | 2·35 | 21·17 | 697 |
| BT1 | $90LiBO_2$–$10TeO_2$ | 2·64 | 23·00 | 683 |
| BT2 | $80LiBO_2$–$20TeO_2$ | 2·95 | 24·31 | 676 |
| BT3 | $70LiBO_2$–$30TeO_2$ | 3·24 | 25·52 | 642 |
| BT4 | $60LiBO_2$–$40TeO_2$ | 3·57 | 26·24 | 621 |
| BT5 | $50LiBO_2$–$50TeO_2$ | 3·87 | 27·05 | 593 |
| BT6 | $40LiBO_2$–$60TeO_2$ | 4·32 | 26·77 | 581 |
| BT7 | $30LiBO_2$–$70TeO_2$ | 4·77 | 26·55 | 576 |
| CT0 | $0LiCl$–$70LiBO_2$–$30TeO_2$ | 3·24 | 25·52 | 642 |
| CT1 | $10LiCl$–$60LiBO_2$–$30TeO_2$ | 3·21 | 25·53 | 639 |
| CT2 | $20LiCl$–$50LiBO_2$–$30TeO_2$ | 3·25 | 24·99 | 625 |
| CT3 | $30LiCl$–$40LiBO_2$–$30TeO_2$ | 3·27 | 24·62 | 618 |
| CT4 | $40LiCl$–$30LiBO_2$–$30TeO_2$ | 3·21 | 24·85 | 610 |
| CL0 | $30LiCl$–$00LiBO_2$–$70TeO_2$ | 4·81 | 25·87 | 550 |
| CL1 | $30LiCl$–$10LiBO_2$–$60TeO_2$ | 4·57 | 24·82 | 549 |
| CL2 | $30LiCl$–$20LiBO_2$–$50TeO_2$ | 4·28 | 23·94 | 546 |
| CL3 | $30LiCl$–$30LiBO_2$–$40TeO_2$ | 3·71 | 24·66 | 529 |
| CL4 | $30LiCl$–$40LiBO_2$–$30TeO_2$ | 3·27 | 24·62 | 618 |
| CL5 | $30LiCl$–$50LiBO_2$–$20TeO_2$ | 2·96 | 23·48 | 642 |
| CL6 | $30LiCl$–$60LiBO_2$–$10TeO_2$ | 2·48 | 23·60 | 630 |
| CL7 | $30LiCl$–$70LiBO_2$–$00TeO_2$ | 2·13 | 22·32 | 620 |

The Fourier transform infrared (FTIR) spectra of the glasses were recorded on a Nicolet 740 FTIR spectrometer. The FTIR transmission spectra were recorded from 4000 to 400 $cm^{-1}$ using KBr pellets containing 2–5 mg of sample.[43] Raman spectra were recorded on a Spex 1403 Raman spectrometer using 514·5 nm radiation from an Argon ion laser (Spectra-Physics Series 2000). The spectra were recorded in the current mode (40 amps) in reflection geometry at 90° incidence using a photo-multiplier tube. All spectra were recorded at room temperature (293 K) on large glass pieces. $^{11}B$ high resolution (HR) magic angle spinning (MAS) nuclear magnetic resonance (NMR) spectra were recorded on a Bruker MSL-300 solid state high resolution spectrometer operating at 90·4 MHz (magnetic field 7·05 T) using a DOTY probe. 90° pulses of 5 μs were employed with a delay time of 10 s between pulses in all the experiments. A spinning speed of 3–7 kHz was employed. All spectra were recorded at room temperature using freshly powdered samples.

## Results and discussion

### *Molar volumes, glass transition temperatures and heat capacities*

The nominal compositions, densities, molar volumes and glass transition temperatures of the three series, BT, CT and CL, of glasses are given in Table 1. The

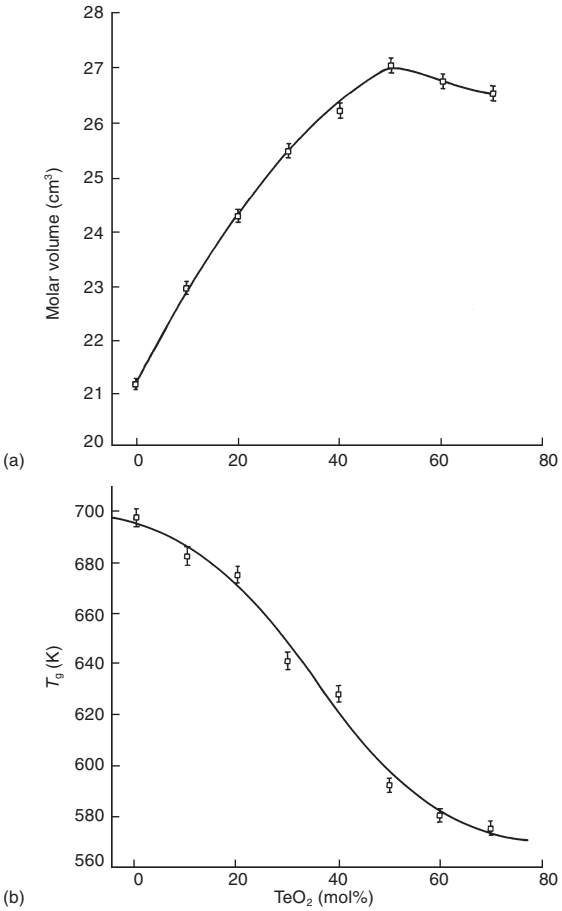


**Figure 2**. *Variation of (a) molar volume and (b) glass transition temperature for BT series of glasses*

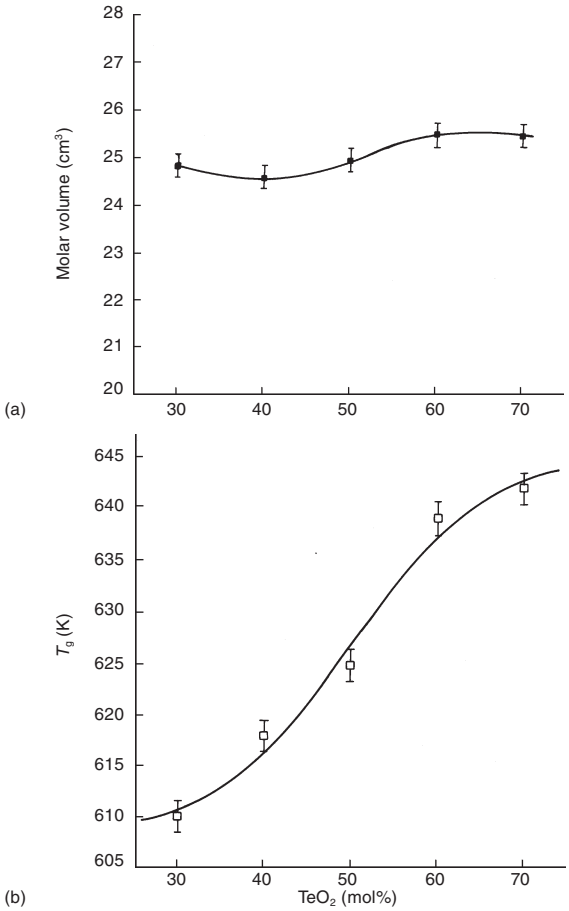


**Figure 3**. *Variation of (a) molar volume and (b) glass transition temperature for CT series of glasses*

variation of molar volumes and glass transition temperatures are shown in Figures 2(a) and (b), respectively, for BT glasses as a function of $TeO_2$ concentration. Similar plots of variations of molar volumes and glass transition temperatures for the CT series (as a function of $LiBO_2$) and CL series (as a function of $TeO_2$) are shown in Figures 3(a) and (b) and 4(a) and (b) respectively. Variation of molar volume in Figure 2(a) indicates that addition of $TeO_2$ tends to increase the volume to about 50 mol% beyond which $V_M$ decreases. The occurrence of the maximum is an indication of structural rearrangements in which the 50 mol% composition is likely to have the most open structure. The molar volume of pure $LiBO_2$ glass (21·17 $cm^3mol^{-1}$) is in fair agreement with earlier values (21·57 $cm^3mol^{-1}$) where the glass was prepared using $Li_2CO_3$ and $H_3BO_3$ as starting materials.[44] Extrapolation gives the volume of pure $TeO_2$ glass as 25·85 $cm^3mol^{-1}$. The glass transition temperature generally decreases with increasing $TeO_2$ concentration. The decrease is somewhat rapid in the region of 20–50 mol% $TeO_2$.

In the CT series of glasses the molar volumes do not vary much for the substitution of $LiBO_2$ by LiCl, the entire variation being under 1·5 $cm^3mol^{-1}$ over the whole composition range. However, a shallow minimum and a shallow maximum occur for the (40:30) and (60:10) combinations of ($LiBO_2$:LiCl), respectively. Substitution of LiCl by $LiBO_2$ leads to an essentially monotonic and almost sigmoidal increase in the glass transition temperatures.

In the CL series, however, the variation of both $V_M$ and $T_g$, Figures 4(a) and (b), are rather complex. Up to 30 mol% substitution by $TeO_2$, the molar volume shows an increasing trend. A similar increase is noted in the molar volume above 50 mol% $TeO_2$. But in the region between 30 and 50 mol% $TeO_2$ the molar volume variation exhibits an anomalous decrease. The glass transition temperatures also exhibit remarkable behaviour. While up to 20 mol% substitution of $LiBO_2$ by $TeO_2$ leads to an increase in $T_g$, there is a sudden decrease in $T_g$ around 30 mol% $TeO_2$. $T_g$ again exhibits a slight increase until all the $LiBO_2$ is substituted by $TeO_2$. The $T_g$ behaviour of the 30 mol% $TeO_2$ glass exhibited a large scatter in $T_g$ and was found to be not very reproducible.

The somewhat smooth change in $V_M$ and $T_g$ observed in the BT series is disrupted by the presence of LiCl in the CL series. Therefore, LiCl plays a nontrivial role (not just addition of its own volume) in $V_M$ and $T_g$ variations. This is even more clearly demonstrated in the insets of the Figures 4(a) and (b) where we have plotted the variations of $V_M$ and $T_g$ as functions of $TeO_2$ for only the $LiBO_2$–$TeO_2$ glass portion in them. This is done by first subtracting a constant volume of 7·8 $cm^3$ for 0·3 mol LiCl (it is assumed that molar volume of hypothetical LiCl glass at 298 K≈volume of LiCl melt (900–1050 K) at two-thirds its melting point (589 K))[45] from all the $V_M$ values and by disregarding LiCl in the composition representation. For example the CL2 glass, i.e.

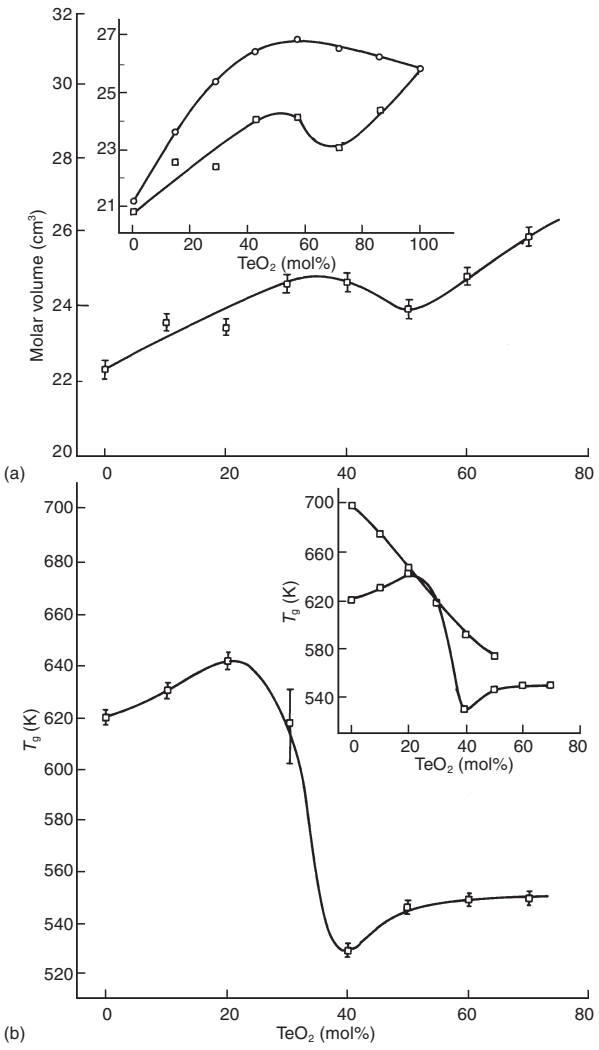


**Figure 4**. *Variation of (a) molar volume and (b) glass transition temperature for CL series of glasses*

$30LiCl.20LiBO_2.50TeO_2$, is represented as 20:50≡(20/0·7):(50/0·7)≡$28{\cdot}57LiBO_2$:$71{\cdot}43TeO_2$). On comparing the variation of $V_M$ in the inset with the same in Figure 2(a), the fact that LiCl influences $V_M$ is quite evident.

Heat capacity plots for the three different series of glasses are shown in Figures 5(a), (b) and (c). Compositions like BT0, BT3, BT6 and CL6 exhibit pre-transition endotherms which we attribute to insufficient annealing. However, the $\Delta C_P$ values have been calculated by extrapolation from lower temperatures in the plot. The CL6 glass exhibits a rather large spread of glass transition temperature, while other glasses in the same series exhibit fairly sharp rise in heat capacities in the transition region. Tellurite rich glasses in the BT series do not exhibit the characteristic humps and also their heat capacities continue to rise in the post glass transition region suggesting continuing degradation of the covalently bonded tellurite network even above $T_g$.

### *IR spectra*

Infrared spectra of the three series of glasses are shown in Figures 6(a), (b) and (c), respectively, for the BT, CT and CL series. The BT0 spectra bears the signature of

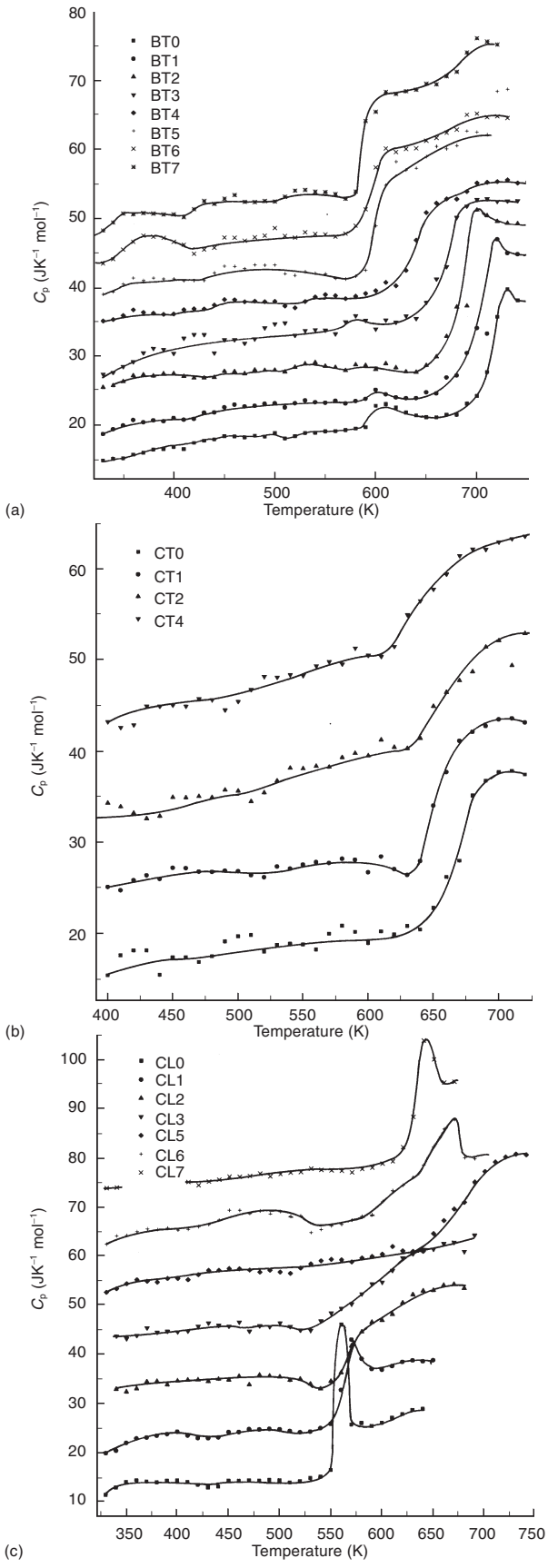


**Figure 5**. *Variation of heat capacity as a function temperature for (a) BT series, (b) CT series and (c) CL series of glasses. (An increment of 10 $JK^{-1}mol^{-1}$ is given to each of the glasses on the Y-axis for clarity)*

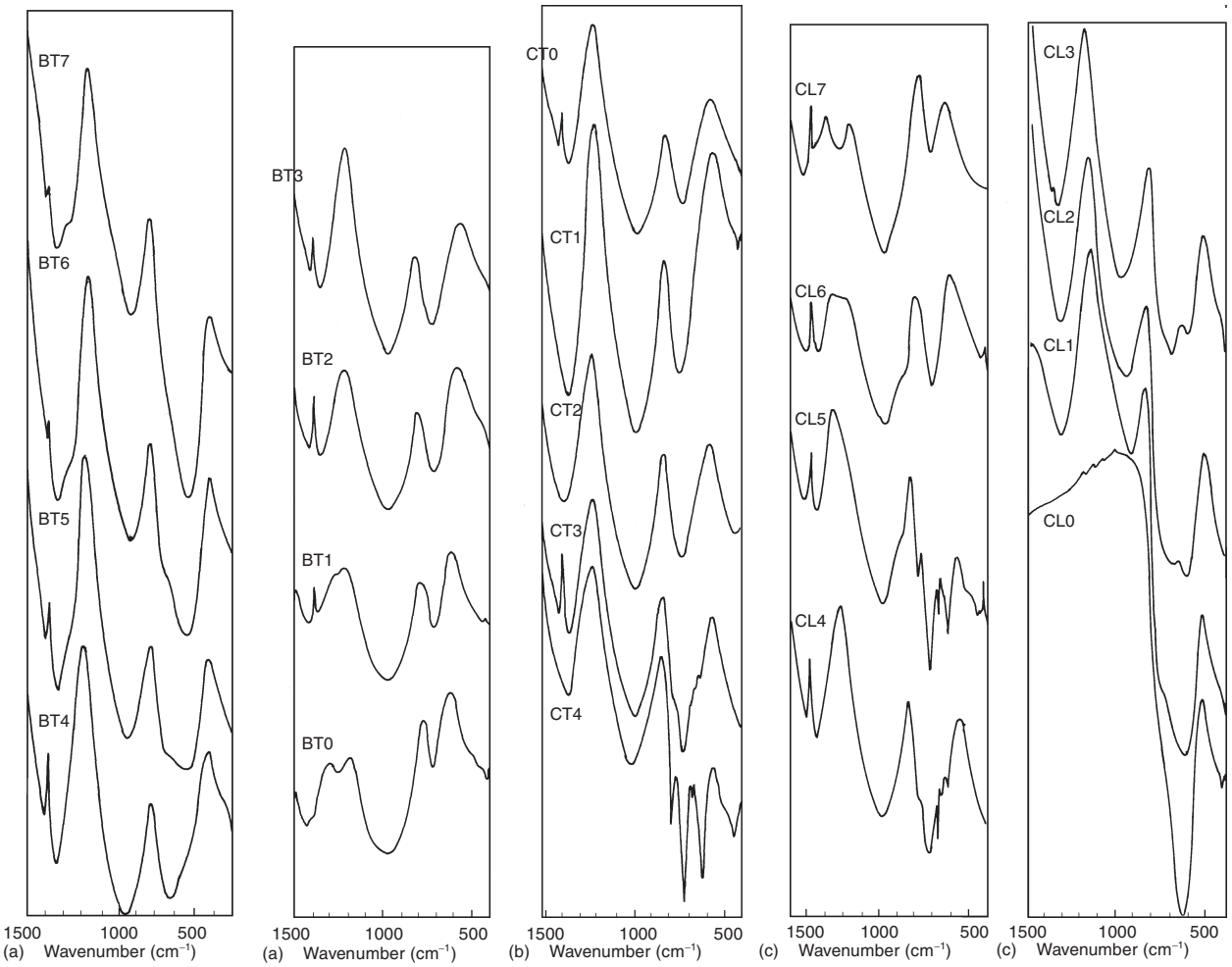


**Figure 6**. *Infrared spectra of (a) BT series, (b) CT series and (c) CL series of glasses*

tetrahedral and trigonal borons in the region of 1000 and 1400 $cm^{-1}$, respectively. The B–O–B bending mode in the region of 700 $cm^{-1}$ is also seen in the BT0. In the BT7, where the spectra is dominated by $TeO_2$, one observes a rather intense peak at ~700 $cm^{-1}$ with a shoulder on the high frequency side but with the characteristic 1000 $cm^{-1}$ (tetrahedral, $B_4$) and 1400 $cm^{-1}$ (trigonal, $B_3$) borate peaks present with a relatively lower intensity. The relative intensities of the $B_4$ and $B_3$ peaks decrease in the intermediate compositions in relation to the 700 –800 $cm^{-1}$ peak of tellurite groups, which increases towards BT7. The B–O–B bending vibration, whose contribution to the spectral intensity of the glasses towards BT7 is expected to decrease, is however subsumed in the characteristic tellurite peak. In the tellurite rich glasses, the trigonal boron peak splits into sub-peaks suggesting the presence of different trigonal species.

Infrared spectra of the CT series glasses are roughly similar to those in BT series. As $LiBO_2$ concentration decreases, the relative intensity in the $TeO_2$ region becomes prominent. But the spectra of CT3 and CT4 glasses reveal that increased percentages of LiCl affect the spectra in the region of 600–900 $cm^{-1}$ significantly and the evolution of different tellurite species is suggested by the changes (see later).

In the CL series the spectra of CL0 is simply that of tellurite glass diluted by the largely infrared inactive LiCl. There is a sharp resonance at 635 $cm^{-1}$ and a shoulder at 770 $cm^{-1}$. But as more and more $LiBO_2$ is added and the glass becomes more and more dilute with respect to $TeO_2$, the $TeO_2$ region of the spectra (600–800 $cm^{-1}$) is marked by evolution of distinct peaks. CL7 spectra reveals that LiCl affects the spectral region corresponding to trigonal borates also. The 1227 $cm^{-1}$ feature is unique to this glass and we refer to it later.

*Raman spectra*

Raman spectra of the glasses are shown in Figures 7(a), (b) and (c) respectively for the BT, CT and CL series of glasses. The spectrum of BT0 corresponds to that of pure $LiBO_2$ glass. It consists of four well defined peaks at 1475, 975, 780 and 530 $cm^{-1}$. The 780 $cm^{-1}$ peak is the most intense in the spectra and is attributed to the presence of four coordinated, $B_4$ borons. Substitution of $LiBO_2$ by $TeO_2$ results in two notable changes. First, the higher frequency scattering at 1475 and 965 $cm^{-1}$ and also the one at 530 $cm^{-1}$ get suppressed. Second, the 780 $cm^{-1}$ peak intensifies by virtue of additional scattering in the same region from tellurite species. In the spectra of intermediate compositions, from BT3 to BT7 glasses, a shoulder in the low frequency region around 680 $cm^{-1}$ emerges which

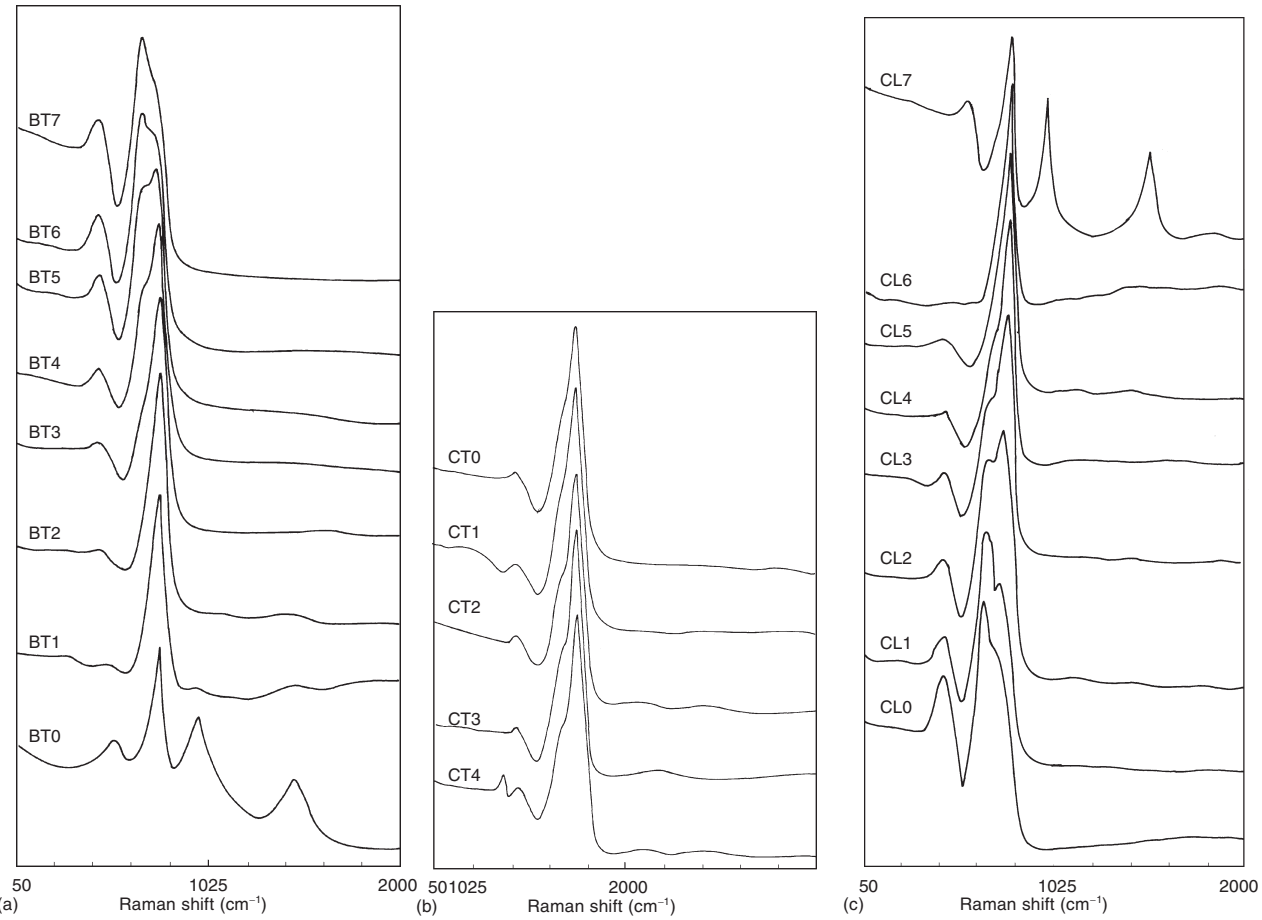


**Figure 7**. *Raman spectra of (a) BT series, (b) CT series and (c) CL series of glasses*

eventually dominates so much that the 780 $cm^{-1}$ scattering appears like a shoulder in the spectra of BT7 glass. A new feature in the 470–490 $cm^{-1}$ region also becomes dominant in these glasses which correlates with increasing presence of $TeO_2$.

The Raman spectra of the CT series reflect essentially the same features, except that in the low frequency region for the high LiCl containing CT4 there is a small feature in the 380–400 $cm^{-1}$ region. This is likely to arise from the rattling (cage vibrational) modes of $Li^+$ ions in their sites.

Effect of substitution of $LiBO_2$ by $TeO_2$ on the absorption peaks in 700–800 $cm^{-1}$ region is clearly evident in the Raman spectra of CL glasses. While borate rich glasses show a unique sharp peak, they evolve into composites of two distinct scatterings due to the presence of borate and tellurite groups. In the CL0 glass containing only tellurite, the two peak character is indicative of the presence of two tellurite species, one of which scatters almost around the same frequency as the borate species, namely 740 $cm^{-1}$. It also suggests that the absorption at 460 $cm^{-1}$ is clearly due to some bending mode in tellurite units.

### *$^{11}B$ HRMAS NMR spectra*

$^{11}B$ HRMAS NMR spectra of the three series of glasses are shown in Figures 8(a), (b) and (c) respectively for the BT, CT and CL glasses. All show sharp resonances due to tetrahedral boron located roughly at the centre of the quadrupolar split resonance of trigonal borons. In all series side bands are observed and their intensities are low. The areas under the tetrahedral and trigonal boron signals were determined as well as the relative proportions of the tetrahedral boron ($N_4=[B_4]/\{[B_3]+[B_4]\}$). These $N_4$ values have been plotted as a function of reduced $LiBO_2$ concentration, $R=([LiBO_2]/\{[LiBO_2]+[TeO_2]\})$ for all three series of glasses in Figures 9(a), (b) and (c), respectively. There is some amount of scatter in the $N_4$ values in the BT series. The scatter is much less in the other two series. All three series of glasses uniformly exhibit high values of $N_4$, the maxima being as high as 0·63 in the BT series and 0·59 and 0·58 respectively in the CT and CL series. It may also be noted that pure $LiBO_2$ glass in the BT series exhibits an $N_4$ value of 0·46, whereas $TeO_2$ free LiCl–$LiBO_2$ glass in the CL series (CL7) has maximum value of about 0·41. Therefore, LiCl may not be responsible for increased $N_4$ concentration in these glasses. On the contrary, $TeO_2$ may be directly responsible for pushing up the values of $N_4$. However, the $N_4$ maximum in BT series occurs around $R\approx0{\cdot}8$ (reduced $LiBO_2$ concentration) and at around $R\approx0{\cdot}3$ in the CL series. Therefore, there appears to be some influence of LiCl on $N_4$ concentration contrary to our earlier observation. But we believe that the influence of LiCl on $N_4$ concentration is only indirect and occurs via its influence on the structural preference for *tp* tellurite units in the structure. We discuss this aspect in the following section. The occurrence of $N_4$ maximum in the CT series is also due to the indirect influence of the same nature.

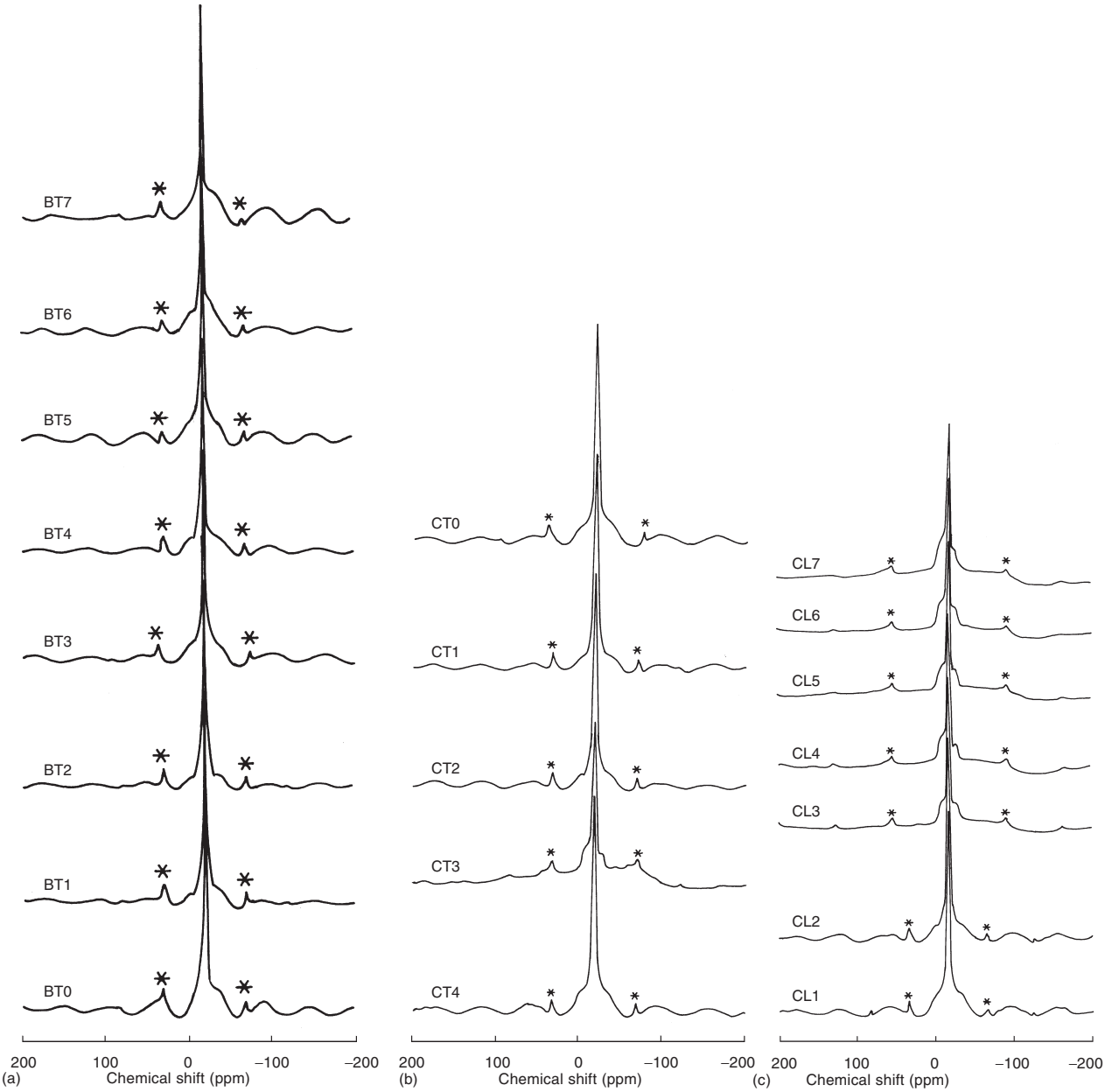


**Figure 8**. *$^{11}B$ HRMAS NMR spectra of (a) BT series, (b) CT series and (c) CL series of glasses*

## The structural model

We first recognise that there are two structural equilibria which influence each other in this rather interesting system of glasses. First is the equilibrium in borate moities as $B_3$ and $B_4$ structural units. Second is the equilibrium of $TeO_2$ moities as $T_4(tbp)$ and $T_3(tp)$ units. All the three spectroscopies, namely infrared, Raman and $^{11}B$ NMR, indicate that with increasing percentage of $TeO_2$, $B_4$ increases. There is a corresponding decrease in $T_4$ units which is not so obvious but the decrease is an essential concomitant as we see below. In pure $TeO_2$ the preferred structural units are $T_4^0$ (superscripts indicate the charge). The structural units in equilibrium in $LiBO_2$ are $B_4^-$ ($[BO_{4/2}]^-$) and $B_3^-$($[BO_{2/2}O]^-$). The experimentally measured $B_3$ in NMR is a sum of $B_3^0$ ($[BO_{3/2}]^0$) and $B_3^-$ units. In pure lithium borate glasses, the $N_4$ maximum occurs at the diborate composition with a value of ~0·5 and corresponds to the ratio $[B_4]^-/\{[B_4]^-+[B_3]^0+[B_3]^-\}$. For $Li_2O/B_2O_3$ ratio greater than unity, $N_4$ decreases approximately linearly. Therefore, in this region, $B_3^0$ is converted into $B_3^-$ by the modifier. $B_4^-$ is also destabilised and converted into $B_3^-$

$$BO_{4/2} \xrightarrow{\text{increased modifier}} BO_{2/2}O$$

Therefore, in $LiBO_2$ ($Li_2O/B_2O_3$=1) we would expect $N_4$ to be less than 0·5. In fact, in pure $LiBO_2$ glass a value of 0·42 is obtained (this value is slightly higher than earlier values[44] obtained in binary $Li_2O$–$B_2O_3$ glasses prepared from $Li_2CO_3$ and $H_3BO_3$. However, we may note that there is a significant scatter in the reported values of $N_4$ in this region).

Therefore the observed increase of $N_4$ in the present system of glasses is possible only if the $Li_2O$:$B_2O_3$ stoichiometry is affected adversely by the presence of $TeO_2$.

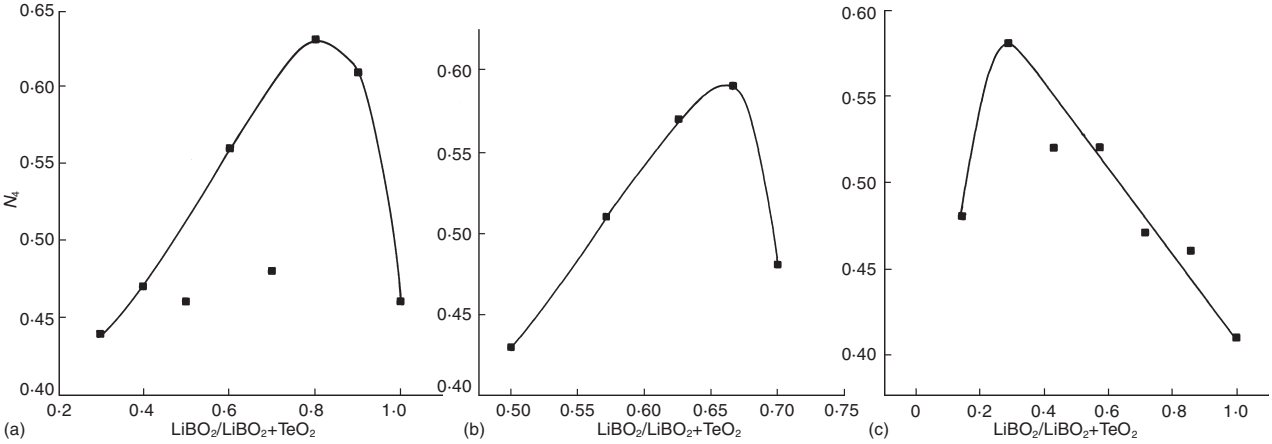


**Figure 9**. *$N_4$ vs reduced $LiBO_2$ concentration (R) for (a) BT series, (b) CT series and (c) CL series of glasses*

A portion of the $Li_2O$ is reclaimed by $TeO_2$ for its own structural modification as follows

$$[BO_{2/2}O]^- + [TeO_{4/2}]^0 \rightarrow [BO_{3/2}]^0 + [TeOO_{1/2}O]^-$$

This reaction is expected to be favoured on simple electronegativity considerations, because the molecular electronegativities[46] of the various species are $[BO_{2/2}O]^-$ {or $[BO_{4/2}]^-$}, 1·96; $[TeO_{4/2}]^0$, 2·92; $[BO_{3/2}]^0$, 2·71; and $[TeO_{3/2}]^-$, 2·22. The electronegativities of the products, {$[BO_{3/2}]^0$ and $[TeO_{3/2}]^-$}, lie between the electronegativities of the reactants, {$[BO_{2/2}O]^-$ and $[TeO_{4/2}]^0$}. Thus, by addition of $TeO_2$ we would expect $Li_2O$ used in modifying $B_2O_3$ to be consumed so that the corresponding $Li_2O/B_2O_3$ ratio also decreases in the glass. Therefore, the equilibrium value of $N_4$ shifts towards larger values. Addition of more $TeO_2$ would not only deplete $Li_2O$ from $LiBO_2$ glass and increase $B_4$, but more importantly tellurite units position themselves between borate units in the structure. The $B_4$ units are thus isolated from other similar borate units in the structure by the intervening tellurite units. This, we believe, exerts a stabilising influence on $B_4^-$ units. Thus we observe that even when R has decreased to only 0·8 at about 20 mol% $TeO_2$, the $N_4$ value reaches a maximum. If $T_4 \rightarrow T_3^-$ conversion alone should drive the $B_3^- \rightarrow B_4^-$ conversion maximum of $N_4$ is expected to occur at R=0·5.

In the CT series also, the maximum of $N_4$ occurs at an R value greater than 0·5 (~0·66) which is lower than in BT series. We will present an argument later in this section that in the presence of LiCl, tellurite units may not be as effective in isolating $B_4$ units. Thus the $B_4$ concentration does not rise as rapidly with $TeO_2$ substitution as in BT series.

In the case of CL series, there is again the effect of LiCl on the equilibrium of tellurite species and hence its influence on the effectiveness of $TeO_2$ on stabilising $B_4$ units. This occurs only after $TeO_2$ concentration exceeds that of LiCl, tellurite units influence the $B_4$ stabilisation and hence peak value of $B_4$ is pushed down to R values of about 0·3.

We should like to address now the structure of the tellurite species in these glasses. The infrared spectra of BT7 and CL0 reveal a remarkable feature regarding the effect of LiCl on the structure of the tellurite species. In BT7 there is no LiCl and there is more $TeO_2$ than $LiBO_2$. There is evidently both $[TeO_{4/2}]^0$ ($T_4^0$) species and $[TeOO_{1/2}O]^-$ ($T_3^-$) units in the glass structure. The $T_4^0$ species gives a band at 635 $cm^{-1}$. The shoulder of this band can be attributed to $T_3^-$ units. In the spectra of CL0, the same band corresponds to $T_4^0$ and $T_3^0$ peaks. The spectra are essentially similar. Therefore, we feel that in the presence of highly ionic components in the glass, such as LiCl, $T_4^0$ units get preferentially transformed into $T_3^0$ units. We further argue that the facile nature of this transformation is because of the small difference in energies of the two species. The chemical binding in $T_4^0$ and $T_3^0$ units can be understood with the help of simple molecular orbital schemes. In both $T_4^0$ and $T_3^0$, the Te atom is assumed to use one *5s*, three *5p* and one *4d* orbital for bonding. $sp^3d$ hybridisation ($d_{z2}$ orbital), gives rise to trigonal bipyramidal, *tbp*, geometry where the lone pair can be accommodated in an equatorial orbital. The other four orbitals form $\sigma$ bonds with *p* (or $sp^3$ hybridised) orbitals of four surrounding oxygens. This accounts well for the $T_4^0$ species. On the other hand, the *5s* with *5p* orbitals on Te can hybridise and give four $sp^3$ hybrid orbitals. The lone pair can be placed in one of them and the three other orbitals are used in bonding to three oxygens. The *4d* orbital can then make a $d\pi$–$p\pi$ type of $\pi$ bond with one of the oxygens which now becomes a double bond. This accounts for the $T_3^0$ species. Although the formation of both $T_4^0$ and $T_3^0$ units use the same set of orbitals, namely $sp^3d$, the nature of the lone pair orbital is different in the two species. In the $T_3^0$ the lone pair orbital is present in a hybridised orbital with a larger *s* contribution. It is likely that $sp^3$ orbital is relatively more stabilised by association with a $Li^+$ ion from LiCl than an $sp^3d$ orbital. This is because the increased *s* character in $sp^3$ orbital gives rise to an enhanced polarisation energy. Further the coulombic interaction in the system is also optimised because the linear polymeric $[TeO_{2/2}O]^0$ chains enable better packing of the constituents. Therefore, the presence of LiCl promotes $T_4^0 \rightarrow T_3^0$ structural transformation (this argument can be extended to $T_4^- \rightarrow T_3^-$ also). Such $T_4 \rightarrow T_3$ conversions in binary alkali tellurites have been well-known in earlier experiments.[22,27,28,31] Therefore, $T_4 \rightarrow T_3$ conversion is a consequence not only of modification in the sense of formation of negatively charged tellurite species, but also is due to addition of highly ionic salts to the glass (like LiCl).

**Table 2**. *Change in connectivities and dimensionalities during modification of borate and tellurate species.*

| *Conversion* | *Change in number of bonds* | *Net change* | *Change in dimensionality* |
|---|---|---|---|
| $B_4^- \rightarrow B_3^0$ | 4→3 | −1 | 3→2 |
| $B_4^- \rightarrow B_3^-$ | 4→2 | −2 | 3→1 |
| $T_4 \rightarrow T_3^-$ | 4→1 | −3 | 3→0 |
| $T_4 \rightarrow T_3^0$ | 4→2 | −2 | 3→1 |

## Glass properties and the model

Simultaneous $B_3 \rightarrow B_4$ and $T_4 \rightarrow T_3$ conversions in the present glass system have profound consequences on the overall structure and thermal properties of these glasses. For example, $B_3^- \rightarrow B_4^-$ conversion brings about a change in structure, from linear (2 covalent linkages) to a 3-dimensional (4 covalent linkages), which increases the volume, thereby creating more open structures. The nature of conversion and the associated change in number of covalent bonds and dimensionality of the structures are summarised in Table 2. We now examine the expected consequences of such structural changes on the properties of the different glasses.

In the BT series, Figure 2(a), the volume increases rapidly with $TeO_2$ addition because of the effect of conversion of $B_3^- \rightarrow B_4^-$ and the formation of $B_3^0$ units. Together, $B_4^-$ and $B_3^0$ create the open network of the borate consisting of an excess of tetrahedrally connected borons. When the ratio of $TeO_2/LiBO_2$ increases to unity this effect $B_3^- \rightarrow B_4^-$ conversion and $B_3^0$ production reaches a maximum. The $TeO_2$ rich region consists of a combination of $T_3^-$, $T_3^0$ and $T_4$ units formed at the expense of $B_3^0$, $B_3^-$ and $B_4^-$ units. This is responsible for the decreasing trend of molar volumes.

In the CT series of glasses the concentration of $TeO_2$ is constant. Therefore the changes in properties are presented as a function of $LiBO_2$ concentration in these glasses, Figure 3(a) and (b). In this series the first member, $40LiCl.30LiBO_2.30TeO_2$ (CT4) glass, already corresponds to a composition of maximum volume originating from $LiBO_2$–$TeO_2$ part of the glass. Further increase of $LiBO_2$ would only increase the concentration of $B_3^-$. Therefore, the volume has a slightly decreasing trend. In the same region the LiCl concentration continues to decrease and therefore the LiCl influence on $T_4 \rightarrow T_3$ conversion decreases. This will manifest in the recovery of $T_4$ units which is reflected in a slightly increasing trend in volumes. At much lower concentration of LiCl (and much higher concentration of $LiBO_2$) the volume change essentially saturates because there are no important structural conversions. This is well reflected in the experiments, Figure 3(a).

The trend in volume change in the CL series (plotted as a function of $TeO_2$ in Figure 4(a)) perhaps represents an acute test of the model (consequences of concentration dependent speciation envisaged in this model). Initially as $TeO_2$ concentration increases, the volume changes are very much the same as in BT series, the volume increases primarily because of the formation of $B_4^-$. Once the ratio of $LiBO_2$ to $TeO_2$ reaches unity (~35 mol% $TeO_2$) the increase in volume reaches a maximum. The next phase of changing volumes is dominated by the breakdown of $T_4^0$ to $T_3^0$ induced by the ionic environment of LiCl. But as $TeO_2$ concentration increases above 50 mol%, $T_4^0 \rightarrow T_3^0$ conversion not only stops but is reversed ($T_4^0$ is regenerated) because there is little $LiBO_2$, and $LiCl/TeO_2$ is much less than unity. The dominant influence of regenerated $T_4^0$ in the structure leads to volume increase in the region 50–70 mol% $TeO_2$. Thus the molar volume behaviour of the glasses in all the three series is completely consistent with the expectation of the model.

The variation of glass transition temperature in the BT series, Figure 2(b), is also consistent with the above model. The $T_g$ of pure $LiBO_2$ glass is highest in BT series. Perhaps this is because of a very efficient packing of $B_3^-$ and $Li^+$ in the structure, so that full advantage is taken by the coulombic interactions. Since the addition of $TeO_2$ rebuilds the more open structure based on $B_4^-$ and also since $T_3^-$ is a large ion, the cohesive energy density in the glass decreases resulting in a rapid decrease in glass transition temperature until 50 mol% addition of $TeO_2$. Above 50 mol% $TeO_2$ it is the $T_4^0$ units which dominate the structural reorganisations, which again leads to a lower energy density and hence lower $T_g$ values. However, the slope of variation of $T_g$ decreases above 50 mol% $TeO_2$.

In the CT series of glasses, Figure 3(b), $T_g$ increase is due to $LiBO_2$ because $TeO_2$ concentration is a constant. As noted earlier, $LiBO_2/TeO_2$ is always greater than unity in this series and ranges between 1·33 and 2·33. The trend is similar to that of BT series for the same region as $TeO_2$ decreases between 0·43 to 0·30. However, LiCl does have its own influence on $T_g$ and can be seen in the extrapolated value of $T_g$ towards 0 mol% $LiBO_2$. Here the $T_g$ should correspond to that of 70LiCl. $30TeO_2$ which is ~590 K. This value is ~$(2/3)T_M$ of LiCl (589 K). Extrapolation of $T_g$ in BT series $T_g$ gives the $T_g$ of pure $TeO_2$ glass as only 530 K. Therefore the $T_g$ is indicative of the influence of the major component in the glass, namely LiCl.

In the CL series the $T_g$ behaviour, Figure 4(b), is rather complex. We offer here a rather tentative explanation. The starting point is the extreme right which corresponds to $LiBO_2$ free LiCl–$TeO_2$ glass (CL0) with a somewhat low $T_g$. Substitution of $TeO_2$ by $LiBO_2$ in this region breaks down the $TeO_2$ structure by converting $T_4^0 \rightarrow T_3^-$. Although $B_4^-$ units are introduced and their concentration is on the rise, the net effect is a weakening of the structure and it pushes down the $T_g$ values to some extent. But around 25 mol% $LiBO_2$ it would generate more than 12·5% $B_4^-$ units which along with $B_3^0$ units creates a 3-dimensional network which permeate the glass structure. It is our speculation that the $T_g$ is controlled by the stronger borate network above this concentration of $LiBO_2$. It is also likely that the inter-penetration of tellurite and borate networks pushes up the $T_g$ to about $50LiBO_2$. Above this composition, $TeO_2$ percentage being small, the $B_4$ content drops (there is more $LiBO_2$), the network strengthening influence of the permeating $TeO_2$ network wanes and the strength of the glass structure decreases. This manifests as a decreasing trend in glass transition. Thus the $T_g$ behaviour can also be considered as broadly consistent with the proposed structural model.

The $\Delta C_P$ values obtained from the heat capacity plots vary widely. In general $\Delta C_P$ values can be related to the configurational excitation entropy on the basis of bond-lattice model.[47,48] The plurality of speciation in these glasses and the associated change in the nature of number of bonds in unit composition makes it difficult to understand quantitatively the $\Delta C_P$ variations and, therefore, these are not discussed any further.

## Conclusions

$LiCl–LiBO_2–TeO_2$ glasses investigated in this paper are characterised by complex structural and bonding variations. On the basis of infrared, Raman and $^{11}B$ HRMAS NMR spectroscopy, it is observed that $TeO_2$ takes away part of the modifier oxide ion from $BO_2$ by virtue of its higher molecular electronegativity. This is followed by a series of structural rearrangements: (1) $[B_4]/\{[B_3]+[B_4]\}$ ratio is pushed in a direction that increase the relative concentration of $B_4$; (2) $TeO_{4/2}$ units, which have *tbp* structure transform into $[TeOO_{1/2}O]^-$ which are *tp* units; (3) $TeO_{4/2}$ units themselves are induced to transform $[TeOO_{2/2}]$ units in the prevailing ionic environment; (4) Addition of LiCl induces the transformation of $T_4 \rightarrow T_3$ units and also favours the stabilisation of $B_4^-$ units. The variation in molar volumes and glass transition temperatures observed in these glasses is well understood on the basis of such changes.

## Acknowledgement

M. Harish Bhat would like to thank the CSIR for financial support.

## References

1. Tanabe, S., Hirao, K. & Soga, N. *J. Non-Cryst. Solids*, 1990, **122** (1), 79.
2. Wang, J. S., Vogel, E. M. & Snitzer, E. *Opt. Mater.*, 1994, **3**, 187.
3. Nasu, H., Matsushita, O., Kamiya, K., Kobayashi, H. & Kubodera, K. *J. Non-Cryst. Solids*, 1990, **124**, 275.
4. Kim, S. H., Yoko, T. & Sakka, S. *J. Am. Ceram. Soc.*, 1993, **76**, 865.
5. Komatsu, T. & Mohri, H. *Phys. Chem. Glasses*, 1999, **40** (5), 257–63.
6. Burger, H., Kneipp, K., Hobert, H., Vogel, W., Kozhukharov, V. & Neov, S. *J. Non-Cryst. Solids*, 1992, **151**, 134.
7. El-Damrawi, G. & Abd-El-Maksoud, S. *Phys. Chem. Glasses*, 2000, **41** (1), 6–9.
8. Akagi, R., Handa, K., Ohtori, N., Hannon, A. C., Tatsumisago, M. & Umesaki, N. *J. Non-Cryst. Solids*, 1999, **256&257**, 111.
9. Sabry, A. I. & El-Samanoudy, M. M. *J. Mater. Sci.*, 1995, **30**, 3930.
10. Mori, H., Igarashi, J. & Sakata, J. *Glastech. Ber.*, 1995, **68**, 327.
11. Blanchandin, S., Marchet, P., Thomas, P., Champarnaud-Mesjard, J. C., Frit, B. & Chagraoui, A. *J. Mater. Sci.*, 1999, **34**, 4285.
12. Arnaudov, M., Dimitrov, V., Dimitriev, Y. & Markova, L. *Mater. Res. Bull.*, 1982, **17**, 1121.
13. Sekiya, T., Mochida, N., Ohtsuka, A. & Tonokawa, M. *J. Ceram. Soc. Jpn.*, 1989, **97**, 1435.
14. Wells, A. F. *Structural inorganic chemistry*. Fourth Edition. 1975. Oxford University Press. Pp 581, 601.
15. Neov, S., Gerasimova, I., Kozhukarov, V., Mikula, P. & Lukas, P. *J. Non-Cryst. Solids*, 1995, **192&193**, 53.
16. Sabadel, J. C., Armand, P., Phillippot, E. & Ibanez, A. *Phys. Chem. Glasses*, 2000, **41** (1), 17–23.
17. Sakida, S., Jin, J & Yoko, T. *Phys. Chem. Glasses*, 2000, **41** (2), 65–70.
18. Shimizugawa, Y., Maeseto, T., Inoue, S. & Nukui, A. *Phys. Chem. Glasses*, 1997, **38** (4), 201–5.
19. Osaka, A., Jianrong, Q., Nanba, T., Takada, J. & Miura, Y. *J. Non-Cryst. Solids*, 1992, **142**, 81.
20. Himei, Y., Miura, Y., Nanba. T. & Osaka, A. *J. Non-Cryst. Solids*, 1997, **211**, 64.
21. Himei, Y., Osaka, A., Nanba. T. & Miura, Y. *J. Non-Cryst. Solids*, 1994, **177**, 164.
22. Ilieva, D., Dimitrov, V, Dimitriev, Y., Bogachev, G. & Krastev, V. *Phys. Chem. Glasses*, 1998, **39** (4), 241–5.
23. Duverger, C., Bouazaoui, M. & Turrell, S. *J. Non-Cryst. Solids*, 1997, **220**, 169.
24. Kneipp, K., Burger, H., Fassler, D. & Vogel, W. *J. Non-Cryst. Solids*, 1984, **65**, 223.
25. Sekiya, T., Mochida, N., Ohtsuka, A. & Soejima, A. *J. Non-Cryst. Solids*, 1992, **151**, 222.
26. Sekiya, T., Mochida, N. & Ohtsuka, A. *J. Non-Cryst. Solids*, 1994, **168**, 106.
27. Tatsumisago, M., Minami, T., Kowada, Y. & Adachi, H. *Phys. Chem. Glasses*, 1994, **35** (2), 89–97.
28. Tatsumisago, M., Lee, S. K., Minami, T. & Kowada, Y. *J. Non-Cryst. Solids*, 1994, **177**, 154.
29. Sekiya, T., Mochida, N., Ohtsuka, A. & Tonokawa, M. *J. Non-Cryst. Solids*, 1992, **144**, 128.
30. Tanaka, K., Yoko, T., Yamada., H. & Kamiya, K. *J. Non-Cryst. Solids*, 1998, **103**, 250.
31. Yoko, T., Kamiya, K., Yamada, H. & Tanaka, K. *J. Am. Ceram. Soc.*, 1988, **71** (2), C-70.
32. Dimitriev, Y., Dimitrov, V. & Arnaudov, M. *J. Mater. Sci.*, 1983, **18**, 1353.
33. Shelby, J. E. *J. Am. Ceram. Soc.*, 1983, **66**, 225.
34. Kuppinger, C. M., Shelby, J. E. *J. Am. Ceram. Soc.*, 1985, **68**, 463.
35. Bray, P. J. *The structure of glass*. Edited by E. Porai-Koshits. 1996. Consultants Bureau, New York.
36. Zhong, J. & Bray, P. J. *J. Non-Cryst. Solids*, 1989, **111**, 67.
37. Abe, T. *J. Am. Ceram. Soc.*, 1952, **35**, 756.
38. Everstein, F., Stevels, J. & Waterman, H. *J. Phys. Chem.*, 1960, **1**, 123.
39. Brückner, R., Chun, H. U., Goretzki, H. & Sammet, M. *J. Non-Cryst. Solids*, 1980, **42**, 49.
40. Park, M. & Bray, P. J. *Phys. Chem. Glasses*, 1972, **13** (2), 50–62.
41. Nishida, T. & Takashima, Y. *J. Non-Cryst. Solids*, 1980, **37**, 37.
42. Bhat, M. H, Kandavel, M. & Rao, K. J. Lithium ion conduction in $LiCl–LiBO_2–TeO_2$ glasses, in preparation.
43. Sathyanarayana, D. N. *Vibrational spectroscopy - theory and applications*. 1996., New Age International Publishers, pp 62–3.
44. Ganguli, M. & Rao, K. J. *J. Phys. Chem.*, 1999, **103**, 920.
45. Janz, G. J. *Molten salts handbook*. 1967. Academic Press, New York. P 39.
46. Sanderson, R. T. *Polar covalence*. 1983. Academic Press, New York.
47. Rao, K. J., & Angell, C. A. *Thermodynamic and relaxational aspects of the glass transition from a bond lattice model. Amorphous materials*.1971. Edited by R. W. Douglas and B. Ellis. John Wiley. P 18.
48. Angell, C. A. & Rao, K. J. *J. Chem. Phys.*, 1972, **57**, 470.